G.D. Manolis
D. Polyzos
Editors

Recent Advances in Boundary Element Methods

A Volume to Honor
Professor Dimitri Beskos

A Semi-Analytical Approach for Boundary Value Problems with Circular Boundaries

Jeng-Tzong Chen, Ying-Te Lee and Wei-Ming Lee

Abstract In this paper, a semi-analytical approach is developed to deal with problems including multiple circular boundaries. The boundary integral approach is utilized in conjunction with degenerate kernel and Fourier series. To fully utilize the circular geometry, the fundamental solutions and the boundary densities are expanded by using degenerate kernels and Fourier series, respectively. Both direct and indirect formulations are proposed. This approach is a semi-analytical approach, since the error stems from the truncation of Fourier series in the implementation. The unknown Fourier coefficients are easily determined by solving a linear algebraic system after using the collocation method and matching the boundary conditions. Five goals: (1) free of calculating principal value, (2) exponential convergence, (3) well-posed algebraic system, (4) elimination of boundary-layer effect and (5) meshless, of the formulation are achieved. The proposed approach is extended to deal with the problems containing multiple circular inclusions. Finally, the general-purpose program in a unified manner is developed for BVPs with circular boundaries. Several examples including the torsion bar, water wave and plate vibration problems are given to demonstrate the validity of the present approach.

1 Introduction

Most of engineering phenomena are simulated by the mathematical models of boundary value problems. In order to solve the boundary value problems, researchers and engineers have paid more attention on the development of boundary integral equation method (BIEM), boundary element method (BEM) and meshless method than domain type methods, finite element method (FEM) and finite difference method (FDM). Although BEM has been involved as an alternative numerical method for solving engineering problems, some critical issues exist, e.g. singular and hypersingular integrals, boundary-layer effect, ill-posed matrix system and mesh generation.

J.-T Chen (✉)

Department of Harbor and River Engineering, National Taiwan Ocean University, Keelung, Taiwan
Department of Mechanical and Mechatronic Engineering,
e-mail: jtchen@mail.ntou.edu.tw

It is well known that BEM is based on the use of fundamental solutions to solve partial differential equations. These functions are two-point functions which are singular as the source and field points coincide. Most of the efforts have been focused on the singular boundary integral equation for problems with ordinary boundaries. In some situations, the singular boundary integral equation is not sufficient to ensure a unique solution, e.g. degenerate boundary, fictitious frequency and spurious eigenvalue. Therefore, the hypersingular equation is required. The applications of hypersingular equations have been summarized in the review article of Chen and Hong (1999).

Unlike the conventional BEM and BIEM, Waterman (1965) introduced first the so-called T-matrix method for electromagnetic scattering problems. Various names, null-field approach or extended boundary condition method (EBCM), have been coined. The null-field approach or T-matrix method was widely used for obtaining numerical solutions of acoustics (Bates and Wall, 1977), elastodynamics (Waterman, 1976) and hydrodynamics (Martin, 1981). Boström (1982) introduced a new method of treating the scattering of transient fields by a bounded obstacle in the three-dimensional space. He defined new sets of time-dependent basis functions, and used these to expand the free-space Green's function and the incoming and scattered fields. The method is a generalization to the time domain of the null-field approach first given by Waterman (1965). A crucial advantage of the null-field approach or T-matrix method consists in the fact that the influence matrix can be computed easily since the singular and hypersingular integrals are avoided. However, they may result in an ill-posed matrix.

In the Fredholm integral equations, the degenerate kernel (or the so-called separate kernel) plays an important role. However, its applications in practical problems seem to have taken a back seat to other methods. The degenerate kernel can be seen as one kind of approximation for the fundamental solution, i.e., the kernel function is expressed as finite sums of products by two linearly independent functions. Kress (1989) proved that the integral equations of the second kind in conjunction with degenerate kernels have the convergence rate of exponential order instead of the linear algebraic order of conventional BEM. Recently, Chen et al. applied the degenerate kernels in conjunction with null-field integral equations to solve many boundary value problems including the Laplace (Chen et al., 2005), Helmholtz (Chen et al., 2007a), biharmonic (Chen et al., 2006) and biHelmholtz (Lee et al., 2007a) problems with holes and/or inclusions. The main gain of their approach is to avoid the improper integrals and free of mesh. They also linked the two numerical methods, Trefftz method and method of fundamental solutions, by using degenerate kernels (Chen et al., 2007b). Therefore, these two methods can be seen to be mathematically equivalent. The similar viewpoint was discussed by Schaback (2007). However, Schaback claimed that MFS is closely connected to the Trefftz method but they are not fully equivalent, since the source points on the far-away filed yield a trial space that is a space of harmonic polynomials (Schaback, 2007). In a word, the degenerate kernel has the property of transferring the integral equation to a linear algebraic system, since the

kernel functions in the integral equations are approximated by using two linearly independent functions.

In this paper, we will apply the semi-analytical approach to deal with engineering problems containing multiple circular boundaries. The boundary integral approach is utilized in conjunction with degenerate kernels and Fourier series. Both direct and indirect formulations will be considered. To fully utilize the circular geometry, the fundamental solutions and the boundary densities are expanded by using degenerate kernels and Fourier series, respectively. This approach is a semi-analytical approach, since the error stems from the truncation of Fourier series in the implementation. Five advantages: (1) free of calculating principal value, (2) exponential convergence, (3) well-posed algebraic system (4) elimination of boundary-layer effect and (5) meshless, of the formulation are the main concern. It will also be extended to deal with the problems containing multiple circular inclusions. Finally, the general-purpose program in a unified manner will be developed for BVPs with circular boundaries. Several examples including the torsion bar, water wave and plate vibration problems are given to see the validity of the present approach.

2 Methods of Solution

2.1 Problem Statements

Suppose a boundary value problem has a domain D which is enclosed with the circular boundary B_k $(k = 0, 1, 2, \ldots, H)$

$$B = \bigcup_{k=0}^{H} B_k \tag{1}$$

as shown in Fig. 1. For the infinite plane problem, the radius a_0 in Fig. 1 is infinite. The governing equation can be expressed by

$$\mathcal{L}u(\mathbf{x}) = 0, \quad \mathbf{x} \in \Omega, \tag{2}$$

where $u(\mathbf{x})$ is the potential function, Ω is the domain of interest and $\mathcal{L}$ denotes the operator for the corresponding problems as shown below:

$$\mathcal{L}u(\mathbf{x}) = \begin{cases} \nabla^2 u(\mathbf{x}) & : \text{Laplacian operator,} \\ (\nabla^2 + k^2)u(\mathbf{x}) & : \text{Helmholtz operator,} \\ (\nabla^4 - \zeta^4)u(\mathbf{x}) & : \text{biHelmholtz operator,} \end{cases} \tag{3}$$

where ∇^2 is the Laplacian operator, k is the wave number which is the angular frequency over the speed of sound and ζ is the frequency parameter.

Fig. 1 Sketch of a circular boundary with circular holes and/or inclusions
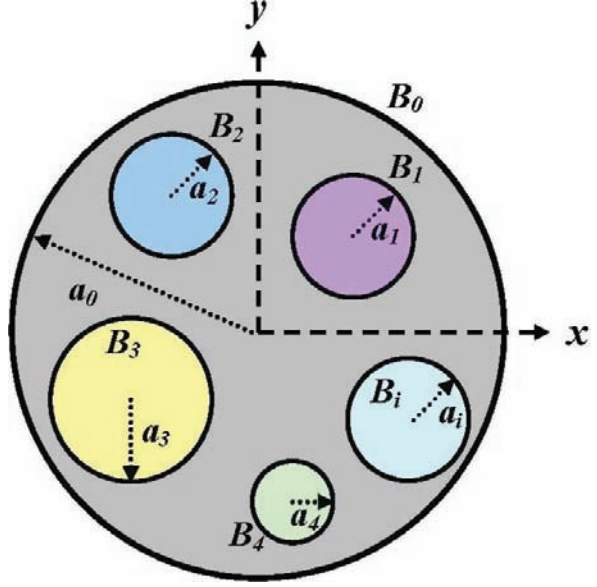
2.2 Dual Null-Field Integral Formulation – the Conventional Version

Based on the dual boundary integral formulation for the domain point, we have

$$2\pi u(x) = \int_B T(s, x)u(s)dB(s) - \int_B U(s, x)t(s)\, dB(s), \quad x \in \Omega, \qquad (4)$$

$$2\pi \frac{\partial u(x)}{\partial n_x} = \int_B M(s, x)u(s)\, dB(s) - \int_B L(s, x)t(s)\, dB(s), \quad x \in \Omega, \qquad (5)$$

where s and x are the source and field points, respectively, B is the boundary, n_x denotes the outward normal vector at field point x, and the kernel function $U(s, x)$ is the fundamental solution which satisfies

$$\mathcal{L}\{U(x, s)\} = \delta(x - s), \qquad (6)$$

in which $\delta(x - s)$ denotes the Dirac-delta function. The other kernel functions are

$$T(s, x) \equiv \frac{\partial U(s, x)}{\partial n_s}, \quad L(s, x) \equiv \frac{\partial U(s, x)}{\partial n_x},$$
$$M(s, x) \equiv \frac{\partial^2 U(s, x)}{\partial n_s \partial n_x}, \qquad (7)$$

where n_s denotes the outward normal vector of the source point s. By moving the field point x to the boundary, the dual boundary integral equations for the boundary point can be obtained as follows:

$$\pi u(x) = C.P.V. \int_B T(s, x)u(s)dB(s)$$

$$- R.P.V. \int_B U(s, x)t(s)dB(s), \quad x \in B, \tag{8}$$

$$\pi \frac{\partial u(x)}{\partial n_x} = H.P.V. \int_B M(s, x)u(s)dB(s)$$

$$- C.P.V. \int_B L(s, x)t(s)dB(s), \quad x \in B, \tag{9}$$

where the $R.P.V.$ is the Riemann principal value, $C.P.V.$ is the Cauchy principal value and $H.P.V.$ is the Hadamard (or called Mangler) principal value. The dual null-field integral equations are

$$0 = \int_B T(s, x)u(s)dB(s) - \int_B U(s, x)t(s)dB(s), \quad x \in \Omega^c, \tag{10}$$

$$0 = \int_B M(s, x)u(s)dB(s) - \int_B L(s, x)t(s)dB(s), \quad x \in \Omega^c, \tag{11}$$

when the field point x is moved to the complementary domain, and the superscript "c" denotes the complementary domain.

2.3 Dual Null-Field Integral Formulation – the Present Version (Direct BIEM)

By introducing the degenerate kernels, the collocation point can be exactly located on the real boundary free of facing singularity. Therefore, the representations of integral equations including the boundary point can be written as

$$2\pi u(x) = \int_B T^E(s, x)u(s)\, dB(s) - \int_B U^E(s, x)t(s)\, dB(s), \quad x \in \Omega \cup B, \tag{12}$$

$$2\pi \frac{\partial u(x)}{\partial n_x} = \int_B M^E(s, x)u(s)\, dB(s) - \int_B L^E(s, x)t(s)\, dB(s), \quad x \in \Omega \cup B, \tag{13}$$

and

$$0 = \int_B T^I(s, x)u(s)dB(s) - \int_B U^I(s, x)t(s)dB(s), \quad x \in \Omega^c \cup B, \tag{14}$$

$$0 = \int_B M^I(s, x)u(s)dB(s) - \int_B L^I(s, x)t(s)dB(s), \quad x \in \Omega^c \cup B, \tag{15}$$

once each kernel is expressed in terms of an appropriate degenerate form (I and E superscripts denote the difference). Here, we used the formulation of potential problem to illustrate the validity of our approach. The more detailed formulation for plate can be consulted with Lee et al. (2007a).

2.4 Indirect Boundary Integral Formulation

Based on the indirect boundary integral formulation, the potential and its derivative can be represented by

$$u(x) = \int_B P(s, x)\phi(s)dB(s), \tag{16}$$

$$\frac{\partial u(x)}{\partial n_x} = \int_B \frac{\partial P(s, x)}{\partial n_x}\phi(s)dB(s), \tag{17}$$

where $U(s, x)$ or $T(s, x)$ is chosen as $P(s, x)$, $\phi(s)$ is the unknown fictitious density distribution. By matching the boundary condition, the unknown fictitious density can be obtained. Therefore, the potential in the field is determined by using the Eq. (16). The extended application to plate problems can be found in Lee et al. (2007a). The comparison of direct and indirect approaches is shown in Table 1. It must be noted that the null-field equation is not available in the indirect formulation.

Table 1 Comparison of direct and indirect BIEMs

	Direct BIEM	Indirect BIEM
Null field	◯	N. A.
Approach	UT (singular equation) LM (hypersingular equation)	$\begin{pmatrix} U \\ L \end{pmatrix}$ (single layer) $\begin{pmatrix} T \\ M \end{pmatrix}$ (double layer)
Singularity	Disappear	Disappear

2.5 Expansions of the Fundamental Solution and Boundary Density

The closed-form fundamental solutions as mentioned above are

$$U(\mathbf{s}, \mathbf{x}) = \begin{cases} \frac{1}{2\pi}\ln r & \text{for the Laplace problem} \\ \frac{i}{4}H_0^{(1)}(kr) & \text{for the Helmholtz problem} \\ \frac{1}{8\zeta^2}[Y_0(\zeta r) + i J_0(\zeta r) + \frac{2}{\pi}(K_0(\zeta r) + i I_0(\zeta r))] & \text{for the biHelmholtz problem} \end{cases}$$

$$\tag{18}$$

where $r \equiv |s - x|$ is the distance between the source point and the field point, i is the imaginary number ($i^2 = -1$), $H_0^{(1)}$ is the first kind Hankel function of the zeroth order, $J_0(\zeta r)$ and $Y_0(\zeta r)$ are the first kind and second kind Bessel functions of the zeroth order, respectively, $I_0(\zeta r)$ and $K_0(\zeta r)$ are the first kind and second kind modified Bessel functions of the zeroth order, respectively. To fully utilize the property of circular geometry, the mathematical tools, separable kernel (or so-called degenerate kernel) and Fourier series, are utilized for analytical integrations.

2.5.1 Degenerate (Separable) Kernel for Fundamental Solutions

By employing the separating technique for source point and field point, the kernel function $U(s, x)$ can be expanded in terms of degenerate (separable) kernel in a series form as shown below:

$$U(s, x) = \begin{cases} U^I(s, x) = \sum_{j=0}^{\infty} A_j(s)B_j(x), & |x| \leq |s|, \\ U^E(s, x) = \sum_{j=0}^{\infty} A_j(x)B_j(s), & |x| > |s|, \end{cases} \tag{19}$$

where the superscripts "I" and "E" denote the interior and exterior cases, respectively. The other kernels in the boundary integral equation can be obtained by utilizing the operators of Eq. (7) with respect to the kernel $U(s, x)$. When the degenerate kernel is used, we choose two linearly independent sets of $\{A_j\}$ and $\{B_j\}$. In the computation, the degenerate kernel can be expressed as finite sums of products of functions of s alone and functions of x alone. Equation (19) is valid for one, two and three dimensional cases as shown in Fig. 2. In this paper, we focus on two-dimensional problems. The degenerate kernels for the fundamental solutions of the three operators are shown in Chen et al. (2005, 2007), and Lee et al. (2007a).
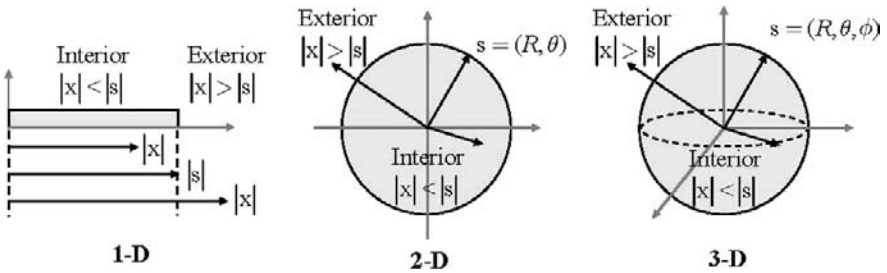

Fig. 2 Degenerate kernel for the one, two and three dimensional problems

2.5.2 Fourier Series Expansion for Boundary Densities

We apply the Fourier series expansion to approximate the boundary potential and its normal derivative as expressed by

$$u(s) = a_0 + \sum_{n=1}^{\infty} a_n \cos n\theta + b_n \sin n\theta, \quad s \in B, \tag{20}$$

$$t(s) = p_0 + \sum_{n=1}^{\infty} p_n \cos n\theta + q_n \sin n\theta, \quad s \in B, \tag{21}$$

where a_n, b_n, p_n and q_n ($n = 0, 1, 2, \ldots$) are the Fourier coefficients and θ is the polar angle. In the real computation, the integrations can be analytically calculated by employing the orthogonal property of Fourier series and only the finite M number of terms is used in the summation. The present method belongs to one kind of semi-analytical methods since error only attributes to the truncation of Fourier series.

2.6 Adaptive Observer System

After collocating points in the null-field integral equation of Eq. (14), the boundary integrals through all the circular contours are required. Since the boundary integral equations are frame indifferent (i.e. rule of objectivity), the origin of the observer system can be adaptively located on the center of the corresponding boundary contour under integration. Adaptive observer system is chosen to fully employ the circular property by expanding the kernels into degenerate forms. Fig. 3 shows the boundary integration for the circular boundaries in the adaptive observer system. The dummy variable in the circular contour integration is the angle (θ) instead of radial coordinate (R). By using the adaptive system, all the boundary integrals can be determined analytically free of principal value senses.
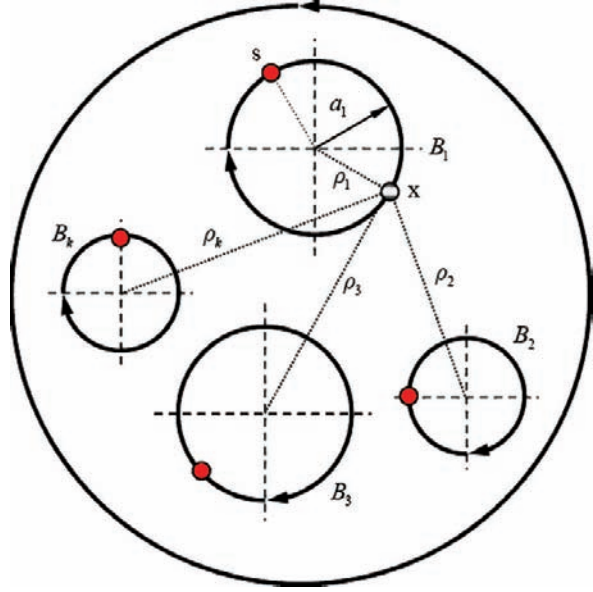
2.7 Linear Algebraic Equation

In order to calculate the Fourier coefficients, N ($N = 2M + 1$) boundary nodes for each circular boundary are needed and they are uniformly collocated on each circular boundary. From Eqs. (14) and (15), we have

$$0 = \sum_{j=0}^{H} \int_{B_j} T(s, x) u(s) \, dB(s) - \sum_{j=0}^{H} \int_{B_j} U(s, x) t(s) \, dB(s), \quad x \in D^c \cup B, \tag{22}$$

$$0 = \sum_{j=0}^{H} \int_{B_j} M(s, x) u(s) \, dB(s) - \sum_{j=0}^{H} \int_{B_j} L(s, x) t(s) \, dB(s), \quad x \in D^c \cup B. \tag{23}$$

It is noted that the integration path is counterclockwise on the outer boundary, others are clockwise. For the B_j integral of the circular boundary, the kernels ($U(s, x)$, $T(s, x)$, $L(s, x)$ and $M(s, x)$) are expressed by degenerate kernels when the circle of observation located is the same as that of integral path. The boundary densities ($u(s)$ and $t(s)$) are substituted by using the Fourier series. The linear algebraic system is obtained

$$[U]\{t\} = [T]\{u\}, \tag{24}$$

where $[U]$ and $[T]$ are the influence matrices with a dimension of $(H+1)\times(2M+1)$ by $(H+1)\times(2M+1)$, $\{u\}$ and $\{t\}$ denote the column vectors of Fourier coefficients with a dimension of $(H + 1) \times (2M + 1)$ by 1. All the unknown coefficients can be calculated by using the linear algebraic equations. Then the unknown boundary data can be determined and the potential is obtained by substituting the boundary data into Eq. (12).

2.8 Transformation of Tensor Components

In order to determine the field of potential gradient, the normal and tangential derivatives should be calculated with care. For the non-concentric case, special treatment for the potential gradient should be taken care as the source and field points locate on different circular boundaries. The detailed tensor transformation is shown in Lee et al. (2007a).

3 Illustrative Examples

Example 1: A circular bar with an eccentric inclusion

A circular bar of radius R_0 with an eccentric circular inclusion of radius R_1 is shown in Fig. 4. The ratio of R_1/R_0 and e_x/R_0 are 0.3 and 0.6, respectively. The torsional rigidity G of cross section is expressed as

$$G = \sum_{k=0}^{H} \mu_k \left[\int_{\Omega} (x^2 + y^2)\, d\Omega - \int_{B_k} \varphi \frac{\partial \varphi}{\partial n} dB_k \right], \qquad (25)$$

where μ_k is the shear modulus of kth inclusion and φ is the warping function. It is found that the solution converges fast by using only fourteen terms of Fourier series. The results of torsional rigidity for various values of μ_1/μ_0 are shown in Table 2. For verifying our results, the exact solution of Muskhelishvili (1953) and
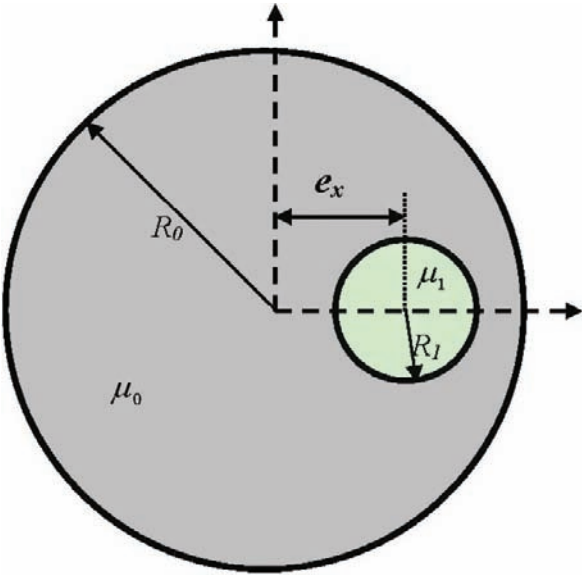

Fig. 4 Sketch of an eccentric circular inclusion problem

Table 2 Torsional rigidity of a circular bar with an eccentric inclusion

$\dfrac{\mu_1}{\mu_0}$	$2G/\pi\mu_0 R_0^4$		
	Muskhelishvili (1953)	Tang (1996)	Present (M=20)
0	0.82370	0.82377	0.82370
0.2	0.89180	0.89181	0.89180
0.6	0.96246	0.96246	0.96246
1.0	1.00000	1.00000	1.00000
5.0	1.10800	1.10794	1.10800
20.0	1.25224	1.25181	1.25224
1000	9.19866	N/A	9.19866

Fig. 5 Interaction of an incident water wave with four cylinders
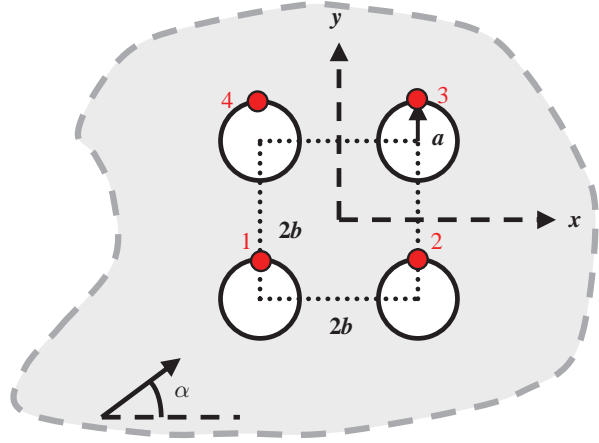
the result of integral equation formulation by Tang (1996) are also shown in Table 2 for comparison. The present results match very well with the exact solution derived by Muskhelishvil and are better than those of Tang (1996).

Example 2: Water wave impinging four cylinders

In this example, we consider a water wave problem by an array of four bottom-mounted vertical rigid circular cylinders with the same radius a located at the vertices of a square $(-b, -b)$, $(-b, b)$, $(b, -b)$, (b, b), respectively, as shown in Fig. 5. Consider the incident wave in the direction of 45 degree ($\alpha = 45°$). The first-order force for four cylinders in the direction of the incident wave is shown in Fig. 6. It is found that the force effect on the cylinder 2 and the cylinder 4 is identical as expected due to symmetry. The maximum free-surface elevation amplitude is plotted in Fig. 7. Also, the results of potentials at the north pole of each cylinder are also compared well with the approximate series solution given by Linton and
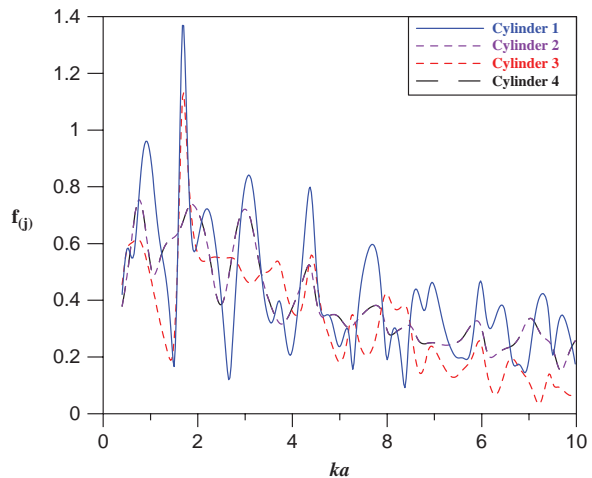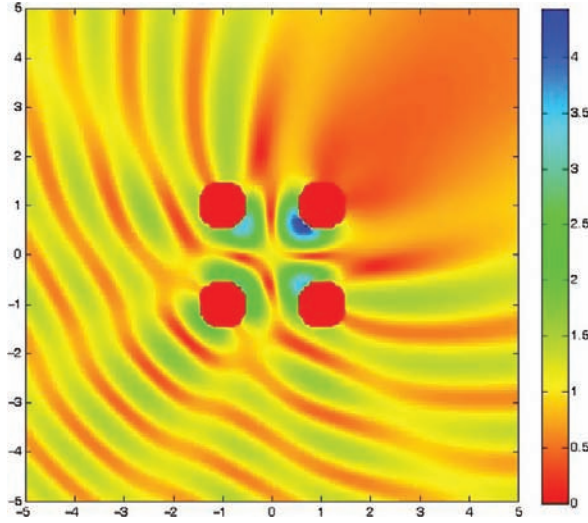

Fig. 6 The first-order force for four cylinders using the proposed method

Fig. 7 Contour of the
maximum free-surface
elevation amplitude

Evans (1990) and the BEM data by Perrey-Debain et al. (2003) as shown in Table 3.
The results agree well with those of Perrey-Debain et al.

Table 3 Potential (ϕ) at the north pole of each cylinder ($ka = 1.7$)

	Present method	Perrey-Debain et al.	Linton & Evan
Cylinder 1	−2.418395851	−2.418395682	−2.418395683
	+0.753719467 i	+0.753719398 i	+0.753719398 i
Cylinder 2	2.328927362	2.328927403	2.328927400
	−0.310367580 i	−0.310367705 i	−0.310367707 i
Cylinder 3	0.350612027	0.350611956	0.350611956
	−0.198852116 i	−0.198852086 i	−0.198852086 i
Cylinder 4	−0.383803194	−0.383803273	−0.383803272
	+1.292792513 i	+1.292792457 i	+1.292792455 i

Example 3: A circular plate with an eccentric hole

A circular plate weakened by an eccentric hole is considered. The offset distance e
of the eccentric hole is 0.45 m ($e/a = 0.45$) as shown in Fig. 8. The FEM model of
the ABAQUS used 8217 elements and 8404 nodes. The former six natural frequency
parameters and modes by using FEM (Khurasia, 1978), ABAQUS and the present
method are shown in Fig. 9. The results of the present method match well with those
of FEM using ABAQUS. In the results of Khurasia (1978), the first mode was not
reported while the second and fourth modes are lost. A little deviation is also shown
in the results reported by Khurasia and Rawtani due to the coarse mesh. Owing to
the lack of stiffness of the clamped boundary condition in reality, it is expected that

Fig. 8 A circular plate with an eccentric hole subject to clamped-free boundary conditions

Case2:

Geometric data:
a=1m
b=0.25m
e=0.45m
Boundary condition:
Inner circle : free
Outer circle: clamped
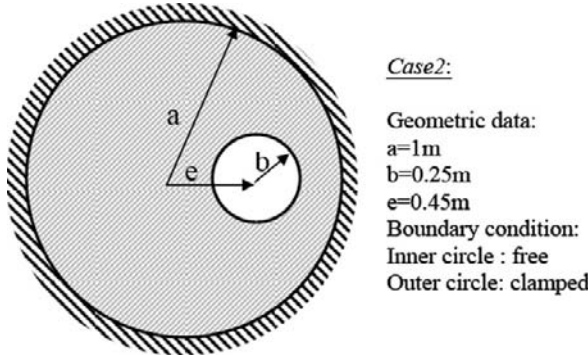
MODE	1	2	3	4	5	6
Present method	3.1870	4.5210	4.7400	5.7580	6.0600	6.2560
ABAQUS	3.2020	4.5300	4.7450	5.7753	6.0899	6.2361
Khurasia and Rawtani 1978	3.1623 <2.8810> N/A	N/A N/A N/A	4.6690 <4.6904>	N/A N/A N/A	5.8138 <5.6391>	6.0828 N/A

Fig. 9 The former six natural frequency parameters and modes of a circular plate with an eccentric hole where <> denotes the experimental data

the experimental data (Khurasia, 1978) are less than those obtained by using the other methods.

4 Conclusions

For the boundary value problems with circular boundaries, we have proposed a null-field BIEM formulation by using degenerate kernels, the null-field integral equation and Fourier series in companion with adaptive observer system and vector decomposition. Three operators for Laplace, Helmholtz and biHelmholtz problems were all considered. This method is a semi-analytical approach for the problems with circular boundaries since only truncation error in the Fourier series is involved. The method shows great generality and versatility for the problems including circular boundaries. Not only the torsion problem but also the water wave as well as

plate vibration problems were solved. Five goals: (1) free of calculating principal value, (2) exponential convergence, (3) well-posed algebraic system, (4) elimination of boundary-layer effect and (5) meshless, of the formulation were achieved. A general-purpose program for solving the problems with arbitrary number, various size and any location of circular cavities and/or inclusions was developed.

References

Bates RHT, Wall DJN (1977) Null field approach to scalar diffraction. I. General method. Philos. Trans. R. Soc. Lond. 287: 45–78

Boström A (1982) Time-dependent scattering by a bounded obstacle in three dimensions. J. Math. Phys. 23: 1444–1450

Chen JT, Hong H-K (1999) Review of dual boundary element methods with emphasis on hypersingular integrals and divergent series. ASME Appl. Mech. Rev. 52: 17–33

Chen JT, Shen WC, Wu AC (2005) Null-field integral equations for stress field around circular holes under anti-plane shear. Eng. Anal. Bound. Elem. 30: 205–217

Chen JT, Hsiao CC, Leu SY (2006) Null-field integral equation approach for plate problems with circular boundaries. ASME J. Appl. Mech. 73: 679–693

Chen JT, Chen CT, Chen PY, Chen IL (2007a) A semi-analytical approach for radiation and scattering problems with circular boundaries. Comput. Meth. Appl. Mech. Eng. 196: 2751–2764

Chen JT, Wu CS, Lee YT, Chen KH (2007b) On the equivalence of the Trefftz method and method of fundamental solution for Laplace and biharmonic equations. Comput. Math. Appl. 53: 851–879

Khurasia HB, Rawtani S (1978) Vibration analysis of circular plates with eccentric hole. ASME J. Appl. Mech. 45: 215–217

Kress R (1989) Linear integral equations. Springer, Berlin

Lee WM, Chen JT, Lee YT (2007a) Free vibration analysis of circular plates with multiple circular holes using indirect BIEMs. J. Sound Vib. 304: 811–830

Lee YT, Chen JT, Chou KS (2007b) Revisit of two classical elasticity problems using the null-field BIE. in APCOM'07 in conjunction with EPMESC XI, Kyoto, Japan

Linton CM, Evans DV (1990) The interaction of waves with arrays of vertical circular cylinders. J. Fluid Mech. 215: 549–569

Martin PA (1981) On the null-field equations for water-wave radiation problems. J. Fluid Mech. 113: 315–332

Muskhelishvili NI (1953) Some basic problems of the mathematical theory of elasticity. Noordhoff, Groningen

Perrey-Debain E, Trevelyan J, Bettess P (2003) Plane wave interpolation in direct collocation boundary element method for radiation and wave scattering: numerical aspects and applications. J. Sound Vib. 261: 839–858

Schaback R (2007) Adaptive Numerical Solution of MFS Systems, in ICCES Special Symposium on Meshless Methods, Patras, Greece

Tang RJ (1996) Torsion theory of the crack cylinder. Shanghai Jiao Tong University Publisher, Shanghai (in Chinese)

Waterman PC (1965) Matrix formulation of electromagnetic scattering. Proc. IEEE. 53: 805–812

Waterman PC (1976) Matrix theory of elastic wave scattering. J. Acoust. Soc. Am. 60: 567–580